Chemical Engineering Journal 164 (2010) 376–382

Contents lists available at ScienceDirect

Chemical Engineering Journal

journal homepage: www.elsevier.com/locate/cej

Fractal formation description of agglomeration in low shear mixer

Eric Rondet[a,*], Michèle Delalonde[a], Thierry Ruiz[b], Jean Pierre Desfours[b]

[a] Laboratoire de Génie des Procédés, Eau et Bioproduits, UMR CIRAD 016, Université Montpellier I, 15 avenue Charles Flahault, B.P. 14491, 34093 Montpellier cedex 5, France
[b] Laboratoire de Génie des Procédés, Eau et Bioproduits, UMR CIRAD 016, Université Montpellier II, c.c. 05, Place Eugène Bataillon, 34095 Montpellier cedex 5, France

ARTICLE INFO

Article history:
Received 7 September 2009
Received in revised form 18 March 2010
Accepted 26 March 2010

Keywords:
Agglomeration
Nucleation
Coalescence
Fractal structuring
Granular matter

ABSTRACT

Three raw granular materials: kaolin, microcrystalline cellulose, and calcium phosphate, usually used in various industrial areas, are wetted and mixed independently with distilled water. Agglomeration in a low shear mixer is then analyzed. The measurements of agglomerates granulometric (d_{25}, d_{50} and d_{75}) and hydro-textural (solid volume fraction, saturation degree and water content) parameters resulting from the wetting/mixing process are carried out. The later are plotted on a phase diagram, called the hydro-textural diagram. This study brings complementary information about the traditional description of agglomeration: (i) the first stage of nucleation represents that during which the fractal growth patterns (the nuclei) are built, (ii) the second stage of growth by coalescence was proven to conform to a fractal structuring behaviour. In low shear conditions, this experimental observation contradicts the classical description of agglomeration insofar as no consolidation phenomena are observed during coalescence.

1. Introduction

Wet granulation is a process widely carried out and consists in agglomerating powder particles in order to increase their size and/or to shape them in agglomerates. These changes present a number of advantages like (i) reduction of dust production, (ii) enhancement of flowability, (iii) bulk density increase, (iv) reduction in segregation phenomenon. In order to increase the industrial yield and control the quality of the end product, many authors interested in the mechanisms of agglomerates formation during kneading. The quantification of process and formulation parameters that influence agglomerate structuring and growth is a challenge.

The wetting of powders leads to wet agglomerates formation which can be describe as an assembly of solid primary particles that adhere to each other by cohesive forces due to liquid bridges (capillary and viscous forces). Currently, three main mechanisms are retained to describe their growth [1]: (i) wetting and nucleation, (ii) coalescence and growth and finally (iii) attrition and breakage. Each of these mechanisms being modulated by the powder characteristics, the nature of added liquid, and the parameters related to the kneading process. Knight [2] underlines the complexity of these agglomerated structures being made up of elements already obtained by agglomeration. Some authors [2,3] focused their work on this aspect by studying the evolution of the bed bulk porosity during agglomerates growth.

The aim of this work is to give a coherent macroscopic description of the granulometric and hydro-textural parameters of the agglomerates during wetting and kneading in a low shear mixer. The hydro-textural properties measured are solid volume fraction, water content and saturation degree. These parameters are plotted on a phase diagram, called hydro-textural diagram, defined by Ruiz et al. [4]. This phase diagram depicts an elaboration path of agglomeration. For each water content, the combination of agglomerates' size and solid volume fraction leads to suggest a description of the agglomerates growth based on a fractal structuring.

2. Theoretical background

Wet agglomerates are multiphase media described as a solid matrix saturated or unsaturated by a liquid phase. Solid volume fraction and liquid saturation degree are two essential parameters to identify their mechanical behaviour [5]. With the applied stress, two parameters can describe the hydro-textural state of agglomerates if their volume is known. These parameters are: agglomerates solid volume fraction (ϕ) and their water content (w) or saturation degree (S). This last is the ratio of the liquid volume to the pore volume of agglomerates. These parameters are defined by the following relations [4]:

$$\phi = \frac{V_s}{V} = \frac{m}{\rho_s^* \cdot V} \tag{1}$$

$$w = \frac{m_w}{m_s} \tag{2}$$

$$S = \frac{V_w}{V - V_s} = \frac{m_w}{\rho_w^* \cdot (V - (m_s/\rho_s^*))} \tag{3}$$

---

[*] Corresponding author. Tel.: +33 467548685; fax: +33 467548649.
E-mail address: eric.rondet@univ-montp1.fr (E. Rondet).

1385-8947/$ – see front matter © 2010 Elsevier B.V. All rights reserved.
doi:10.1016/j.cej.2010.03.069

Nomenclature

A_i	fractal law prefactor
d_s^*	ratio of the solid to the liquid density
d_i	diameter of size fraction *i* [mm]
d_{25}	diameter of 25% (in number) of the population [mm]
d_{50}	median diameter, diameter of 50% (in number) of the population [mm]
d_{75}	diameter of 75% (in number) of the population [mm]
d_{50}^N	nucleus median diameter [mm]
D_f	fractal dimension
ϕ	solid volume fraction
$\phi_{a,i}$	agglomerates solid volume fraction of size fraction *i*
ϕ_N	nucleus solid volume fraction
m_s	solid mass [g]
m_w	water mass [g]
ρ_s^*	solid density
ρ_w^*	water density
S	saturation degree
V	agglomerate apparent volume [cm^3]
V_s	solid volume [cm^3]
V_w	water volume [cm^3]
w	water content
w_N	nucleus water content
w_{sat}	saturation water content
w_P	plastic limit

In these equations, V_s and V_w are respectively the solid phase and the liquid phase volume in the apparent agglomerate volume V; m_s and m_w are the solid and the liquid masses, ρ_s^* and ρ_w^* their true densities. Between the dry and the saturation states, the saturation degree of the agglomerates can be linked with water content by a power law function (Eq. (4)) where n is a coefficient that makes it possible to take into account the deformability of the medium ($n = 1$, for not deformable media):

$$S = \left(\frac{w}{w_{sat}}\right)^n \text{ with } n \leq 1 \text{ and for } w \leq w_{sat} \tag{4}$$

In Eq. (4), w_{sat} is the water content that ensure the saturation of the medium. When the medium is saturated with water ($S = 1$), the relation (1) can be expressed according to the water content:

$$\phi = \frac{1}{1 + d_s^* w_{sat}} \tag{5}$$

where $d_s^* = \rho_s^*/\rho_w^*$. Eq. (5) makes it possible to obtain a curve indicating, for each value of solid volume fraction, the water content ensuring the agglomerates saturation. In the case of an unsaturated medium, Eqs. (1)–(4) lead to Eq. (6) where solid volume fraction only depends on the water content:

$$\phi = \frac{1}{1 + d_s^* w_{sat}^n w^{1-n}} \quad \forall 0 < w < w_{sat} \tag{6}$$

3. Materials and methods

The raw materials chosen for this study are microcrystalline cellulose (Vivapur 102-JRS), kaolin (Cooper) and dibasic calcium phosphates dehydrate (Callipharm). Microcrystalline cellulose is a polymeric powder commonly used in pharmaceutical formulations for wet granulation. Kaolin and dibasic calcium phosphate were chosen for their mineral nature and the smaller size of their particles compared to that of cellulose. All of these raw materials do not significantly swell or dissolve during wetting. The true densities of solid particles are measured with a helium pycnometer 1305 (Micromeretics) for each raw material. The true density values are equal to 1490, 2580, and 2550 kg m^{-3} for microcrystalline cellulose, kaolin and dibasic calcium phosphate dehydrate, respectively. The size distribution measurement was carried out with a laser granulometer Malvern Mastersizer E (Malvern instrument) and gave an

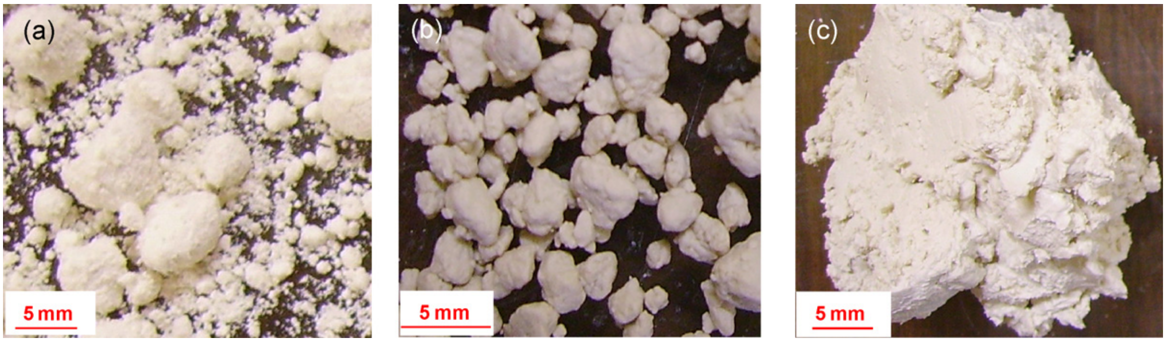

Fig. 1. Morphological evolution of kaolin according to water content: (a) $w = 0.1$, (b) $w = 0.25$ and (c) $w = 0.45$.

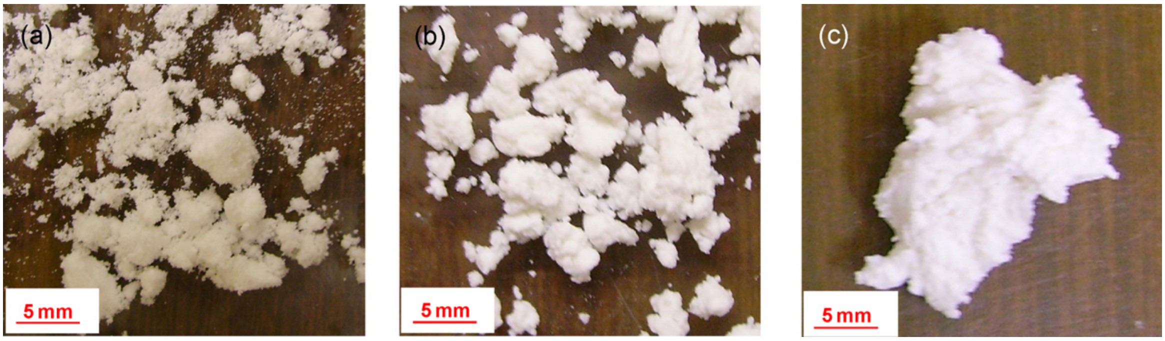

Fig. 2. Morphological evolution of microcrystalline cellulose according to water content: (a) $w = 0.7$, (b) $w = 1.1$ and (c) $w = 1.6$.

Fig. 3. Morphological evolution of calcium phosphate according to water content: (a) $w = 0.11$, (b) $w = 0.21$ and (c) $w = 0.46$.

equivalent volume median diameter (d_{50}) of 112 μm for microcrystalline cellulose, 9.5 μm for kaolin and 12.8 μm for dibasic calcium phosphate dehydrate.

Wet masses are prepared using a planetary mixer (Kenwood Major 1200) with constant rotation speed and dry load, respectively fixed at 70 rpm and 200 g of dry mass. More information about this planetary mixer and impeller dimension can be found in [6]. These operating conditions are mild compared with those of a high shear mixer. The procedure chosen for preparation is tried and tested and is in accordance with previous studies [7,8] related to the extrusion/spheronisation of wet powders in the pharmaceutical field. It ensures the homogenisation of water in the whole volume. During a first mixing period of 3 min, water is steadily sprayed into the mixing thanks to a manual spray. The water volume delivered after each spray has been measured so as to specify the number and also the spraying frequency necessary to obtain the targeted water content. The manual spray generates a size distribution of droplets whose parameters (median diameter = 0.3 mm and dispersion parameter: 0.7) has been measured thanks to an image analysis after spraying water on a surface coated with silicon oil. This wetting stage is followed by a second mixing period of 3 min to ensure optimal distribution. At the end of the mixing stage the wet mass is spread out on a smooth surface. It is constituted of particles and/or agglomerates or pieces of paste depending on the water content. These wetting conditions correspond to an immersion mechanism of nucleation as defined by Schaefer and Mathiesen [9].

Photographs of the spread wet masses are taken (Camera Optio 50L, Pentax) and treated using an image processing software (Image Tool® UTHSCSA) in order to study the evolution of the granulometric parameters. On each photograph, a ruler laid on the smooth surface close to the agglomerates, is used for the measurements calibration. For each water content, granulometric parameters (d_{25}, d_{50}, and d_{75} representing the equivalent surface diameter of 25%, 50% and 75% in number of the measured agglomerates) are seen to become constant for a number of measurements equal to 200. The accuracy of the size measurements is ±0.02 mm. From an experimental point of view, the photographs are divided into five parts (the four corners and the center) where measurements are taken while following a horizontal line to avoid any subjectivity in the choice of the agglomerates to be analyzed. For each agglomerate two measurements are carried out: the circumcircle and the incircle diameters of the agglomerates. As their form generally deviates from that of a sphere, these two measurements must be taken into account in order to obtain a mean diameter. From an experimental point of view, the measurements of hydro-textural parameters are in accordance with the methodology defined by Ruiz et al. [4]. The determination of these parameters (Eqs. (1)–(3)), requires the measurement of three parameters: V, m_w and m_s. Volume measurements are carried out by reading the displaced volume following the introduction into paraffin of one or more agglomerates, weighed beforehand. The volume V is the paraffin displaced volume. Concerning the water content of the immersed agglomerates, it is evaluated thanks to the measurement of m_s and m_w on agglomerates of equivalent size taken in the same wet mass and placed in an oven (105 °C during 24 h).

Plastic limit, which corresponds to Atterberg tests of soil science [10], are carried out in accordance with the French standards (NF P 94-051, 1993). The plastic limit (w_P) is the water content

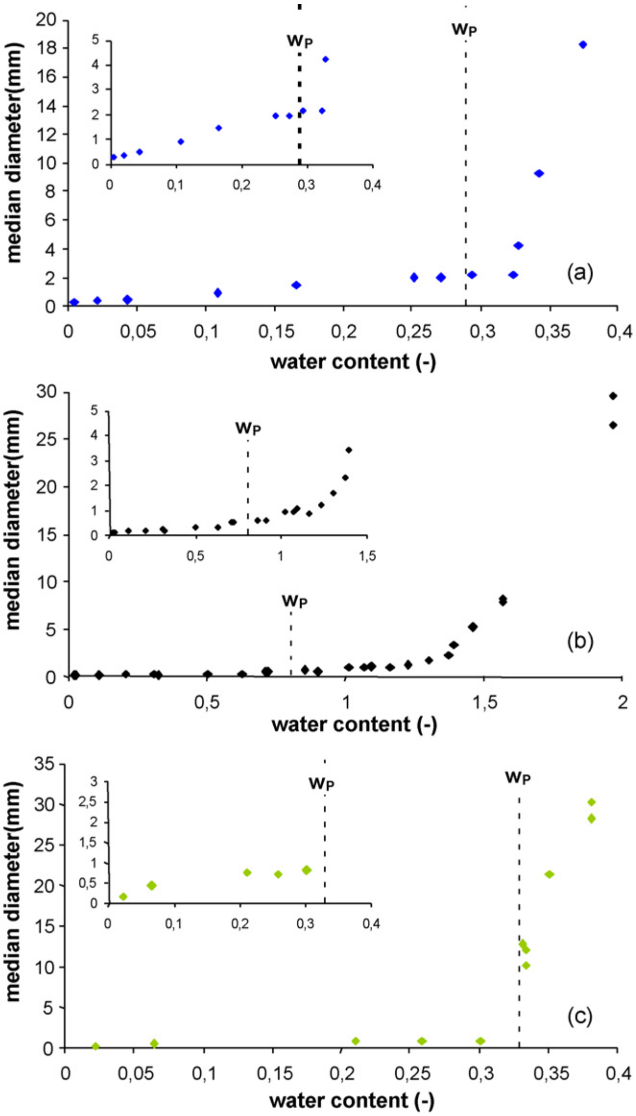

Fig. 4. Median diameter evolution according to water content during agglomeration: (a) kaolin, (b) microcrystalline cellulose and (c) calcium phosphate.

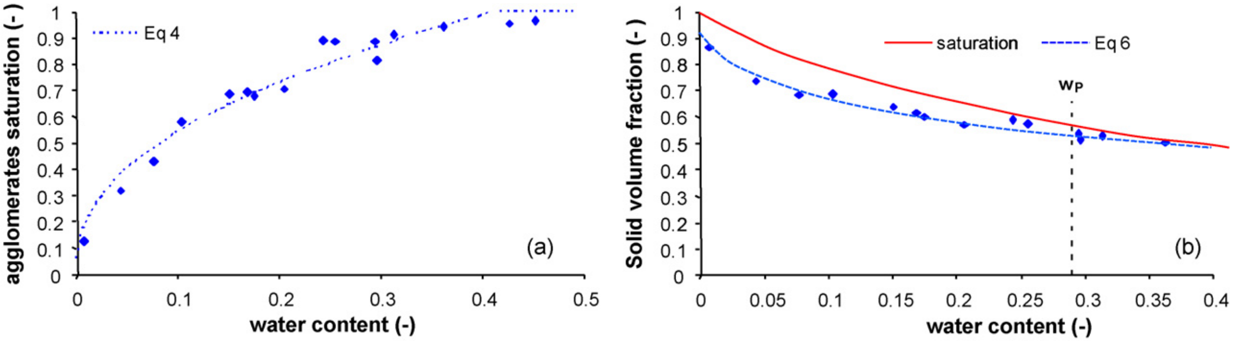

Fig. 5. Hydro-textural evolution of kaolin agglomerates according to water content: (a) saturation degree and (b) solid volume fraction.

transition between the solid and the plastic state. It is the lowest water content at which a cohesive sample can be shaped as a rolled thread with no breaking (3 mm diameter and 10 cm long). The determination of the plastic limit in accordance with this standard is impossible for microcrystalline cellulose which is not a cohesive powder [11]. The values of the plastic limits are respectively equal to 0.29 and 0.33 for kaolin and calcium phosphate.

4. Experimental results, model and discussion

Figs. 1–3 respectively show, for the three raw materials, the changes in the medium state with respect to their water content.

During the wetting of a powder mixing, the aspect of the medium changes drastically. With the addition of the first wetting liquid drops and the effect of the shearing stress, small agglomerates appear. The traditional agglomeration description called “nuclei” these structures obtained at the beginning of wetting [1,12]. When the water content increases, the medium appeared as a bed bulk only made of agglomerates. This water content as well as agglomerates size and shape depends on the nature of the product and process parameters. Though smaller, the calcium phosphate agglomerates are similar to that of kaolin by their form and consistency. The cellulose agglomerates have a more irregular surface and a higher deformability. When the water content is higher than the plastic limit (w_P), the medium gradually changes into a paste whose consistency will depend on the raw material as well as the water content.

For each wetting, the determination of the agglomerates size distribution makes it possible to define the median diameter of the agglomerates (d_{50}). Fig. 4 makes it possible to observe that the median diameter of the agglomerates grows, with respect to the water content, in two main stages: a first monotonous and moderate growth stage, and a second stage of growth where a weak increase in the water content leads to a sharp increase in the median diameter value. The change in the growth mode occurs systematically after the crossing of the plastic limit which corresponds to the water content for which the dough pieces appear.

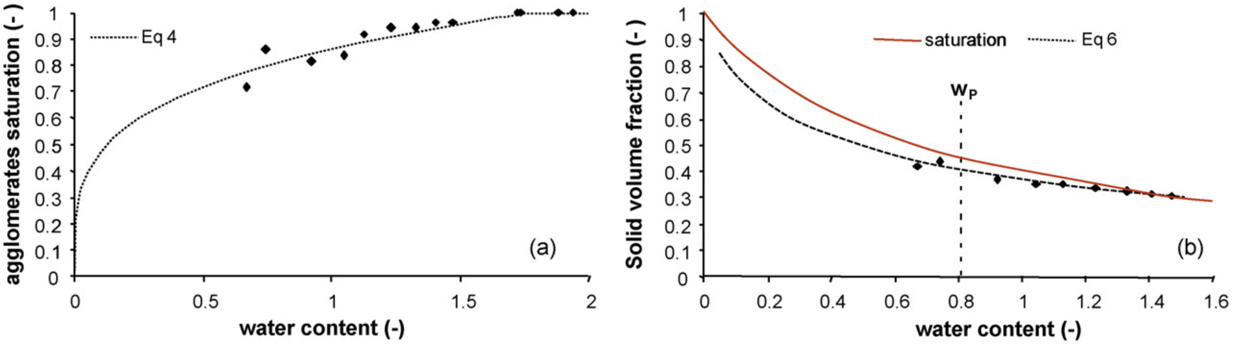

Fig. 6. Hydro-textural evolution of microcrystalline cellulose agglomerates according to water content: (a) saturation degree and (b) solid volume fraction.

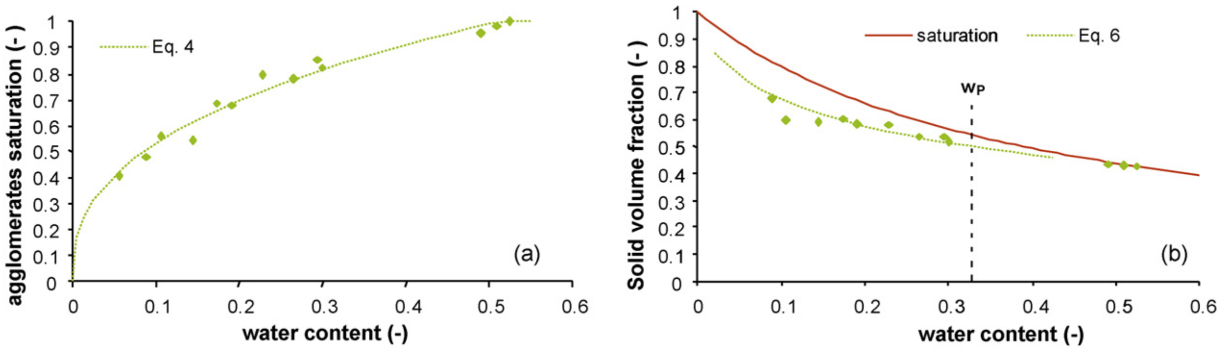

Fig. 7. Hydro-textural evolution of calcium phosphate agglomerates according to water content: (a) saturation degree and (b) solid volume fraction.

Table 1
Values taken by the parameters of Eqs. (4) and (6) for the three products.

	Kaolin	Microcrystalline cellulose	Calcium phosphate
w_{sat}	0.42	1.75	0.51
n	0.43	0.26	0.39
R^2	0.9	0.78	0.92

The agglomerates growth during wetting is associated to changes in solid volume fraction and saturation degree of agglomerates. Figs. 5–7 depict the results of agglomerates immersion in paraffin. It can be pointed out that they saturate gradually as water content increases. This saturation is combined with a reduction in their solid volume fraction. Thus, the experimental data located on the hydro-textural diagram (solid volume fraction *versus* water content [4]) decrease in a monotonous way and join the saturation curve for a water content value (w_{sat}) which is always higher than the plastic limit. It is noted that the paste formation only occurs when agglomerates are close to saturation. Eqs. (4) and (6) make it possible to give an account of the progressive agglomerates saturation and the reduction in their solid volume fraction respectively. Beyond w_{sat}, the agglomerates saturation degree equals 1.

Table 1 summarises the values taken by Eqs. (4) and (6) parameters for each studied raw material. The regression coefficient associated with each model is also mentioned. Concerning w_{sat}, one can observe that its value is always higher than the plastic limit of the considered medium. Nevertheless, these values are really close in the case of kaolin and calcium phosphate if one take into consideration the indetermination on the values of Atterberg limits and w_P especially (±10% [13]).

It can be pointed out in Figs. 5–7 that, for $0 \leq w \leq w_{sat}$, agglomerates coalescence associates an increase in their size and a reduction in their solid volume fraction. From nuclei, the agglomerate growth process integrates progressively more and more porosity along with the increase in water content. From a mathematical point of view, we show that this process is similar to a

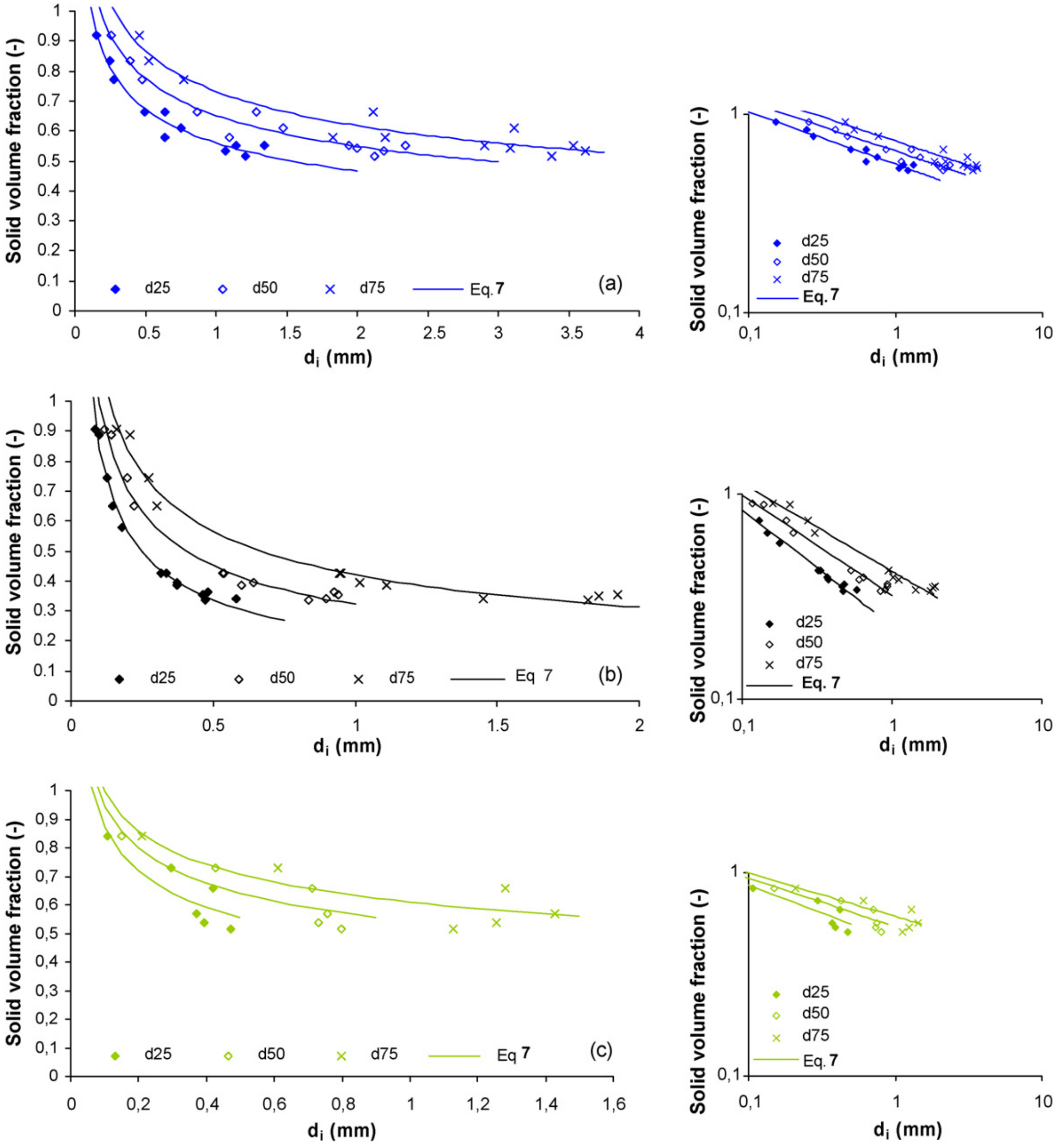

Fig. 8. Fractal behaviour of agglomeration (Log–Log on the right), (a) kaolin, (b) microcrystalline cellulose, and (c) calcium phosphate.

Table 2
Values taken by parameters of Eq. (7) for each studied granulometric fraction of the three raw materials.

	Kaolin	Microcrystalline cellulose	Calcium phosphate
D_f			
d_{25}	2.73	2.43	2.72
d_{50}	2.75	2.51	2.76
d_{75}	2.76	2.57	2.79
Mean	2.75	2.50	2.76
A			
d_{25}	0.56	0.23	0.46
d_{50}	0.65	0.32	0.54
d_{75}	0.73	0.42	0.61
R^2			
d_{25}	0.97	0.99	0.73
d_{50}	0.96	0.94	0.79
d_{75}	0.94	0.99	0.77

fractal structuring [14–17]. The relation between the solid volume fraction and the median diameter makes it possible to define a mass fractal dimension of the agglomerates D_f according to the following equation:

$$\phi_{a,i} = A_i d_i^{Df-3} \tag{7}$$

where $\phi_{a,i}$ is the solid volume fraction and d_i the diameter of the agglomerates.

Fig. 8 shows that Eq. (7) is valid for three size fractions: d_{25}, d_{50}, d_{75}. The curves $\phi_{a,i} = f(d_i)$ are not superposed. This is due to the variation of the prefactor A_i with respect to the size fraction considered. On the other hand, fractal dimension is quite constant for each size fraction (parallel line on the Log–Log scale). Previous works of agglomeration carried out at constant flow rate [18] makes it possible to observe that, for a given water content, the agglomerates characteristics are identical as those observed in our work. Thus the water and time axis can be assimilated and the curves of Fig. 8 can be considered as the result of the analysis of agglomerates characteristics (solid volume fraction and diameter) at different stage during the process of wetting/mixing. It is thus possible to conclude that agglomerates can be considered as structures originated from a fractal formation process, between two characteristic correlation lengths: nuclei diameters (basic pattern) and dough pieces diameter.

The fractal dimension of an object is always lower or equal to the dimension d of the space in which it is considered ($d = 3$ for volumic fractal, $d = 2$ if the fractal is depicted in a plan). This is caused by the fact that the volume of this fractal object cannot grow faster than its diameter raised to the power d. For fractals, the solid volume fraction of the object (ϕ_{ai}) is always a decreasing function of one of its characteristic length (Eq. (7)), that means that its solid volume fraction is asymptotically null, since D_f–d is a negative number. On the other hand, for non-fractal object, those for which $D_f = d$, solid volume fraction is constant. Thus the fractal dimension measurement indicates the more or less dense way in which an object fills space. The closer to 3 (in a 3D space) the fractal dimension is, the more the object is compact [14]. Comparison of fractal dimension values for the three studied products (Table 2) makes it possible to highlight a similarity between kaolin and calcium phosphate. In their case, D_f value is relatively high and close to 2.75. For microcrystalline cellulose, the lower value of D_f (2.5) makes it possible to conclude that the agglomeration process incorporates a higher quantity of porosity than it is the case for the two other products.

If Eq. (7) is applied to nuclei, it becomes Eq. (8):

$$\phi = \phi_N \left(\frac{d_{50}}{d_{50}^N} \right)^{Df-3} \tag{8}$$

Table 3
Values taken by parameters of Eq. (8) for each raw material.

	Kaolin	Microcrystalline cellulose	Calcium phosphate
d_{50}^N	0.27	0.15	0.24
Φ_N	0.92	0.84	0.74
w_N	0.01	0.05	0.06
R^2	0.99	0.85	0.99

where d_{50}^N is the nucleus diameter and ϕ_N its solid volume fraction. This new expression of fractal law makes it possible to define the minimal correlation length giving the validity of Eq. (7): under d_{50}^N, the relation is not justified.

So as to define ϕ_N and d_{50}^N, it is necessary to evaluate the evolution of the particle number in agglomerates during growth. See Rondet's work [18] for more precisions.

Eq. (8) parameters and regression coefficients are summarized in Table 3 for each studied products. In this table, w_N corresponds to the water content related to the nuclei solid volume fraction (ϕ_N). This water content has been calculated according to Eq. (6).

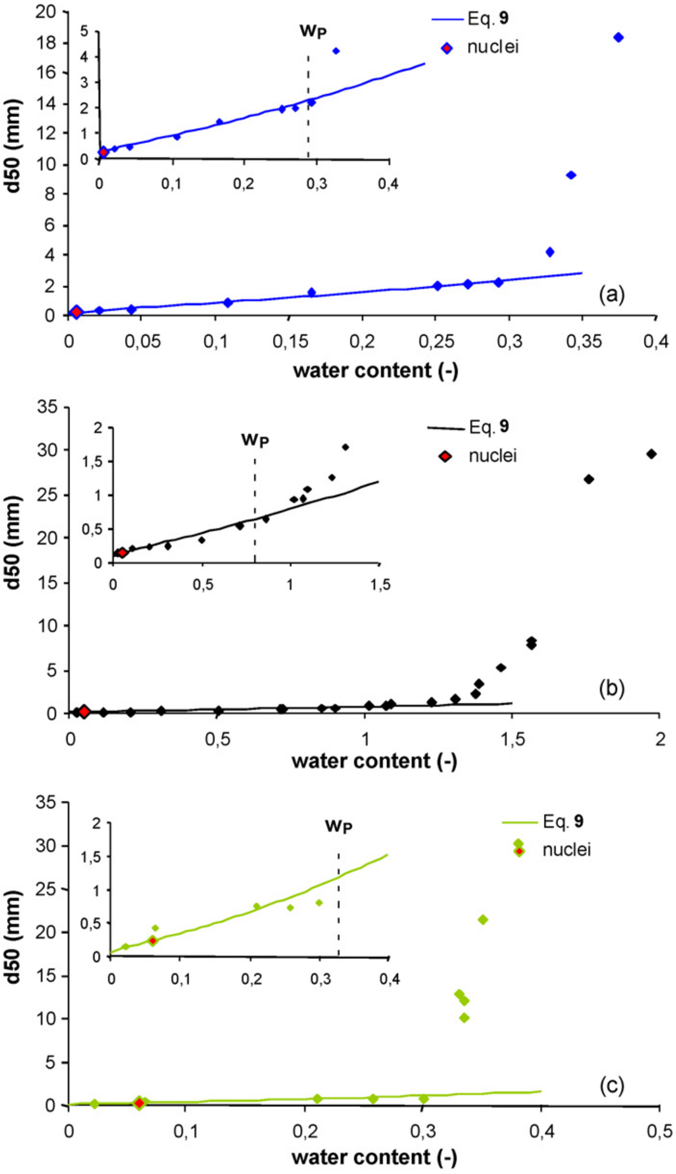

Fig. 9. Fractal model of agglomerates growth (Eq. (9)). (a) Kaolin, (b) microcrystalline cellulose, and (c) calcium phosphate.

Nuclei solid volume fraction ranges between 0.74 and 0.92. Their corresponding water contents are lower or equal to 6%. Nuclei are progressively generated between the dry state and w_N, but they will occupy a representative fraction of the total mixture only starting from this later water content. Thus, w_N is the water content marking the beginning of the agglomeration phenomenon (growth by coalescence). The diameter of the calcium phosphate and kaolin nuclei is close to 250 μm. It is composed of several tens of thousands of particles. Concerning microcrystalline cellulose, the diameter is lower (150 μm) and nucleus only consists of a few units of native particles.

Eqs. (6) and (8) make it possible, thanks to the preliminary determination of n, w_{sat}, D_f, ϕ_N and d_{50}^N, to calculate the evolution of the agglomerates median diameter with respect to the water content:

$$d_{50} = d_{50}^N \left[\frac{1}{\phi_N (1 + d_s^* ({w_{sat}}^n / w^{n-1}))} \right]^{1/(D^f - 3)} \tag{9}$$

Results concerning each studied product are depicted in Fig. 9 in which the calculated point related to nuclei has been added. The median diameter evolution resulting from the fractal analysis of the agglomeration process is completely correlated with experimental data. In the case of polymers and colloids aggregation, the fractal behaviour had already been highlighted and resulted in a successful and profitable theory [15]. Dynamic molecular numerical simulations confirmed the fractal coalescence of this type of elements. This last is due to diffusion and to a total attraction potential (Lennard–Jones potential). The experimental results presented here show that fractal coalescence could be applied to granular matter. In this case, diffusion and Lennard–Jones potential are replaced by ballistic trajectories, initiated by the blades shearing, and a local capillary interaction.

Eq. (9) is valid for water contents under w_{sat}, nevertheless, it is possible to graphically observe that the experimental points of Fig. 9 deviate from the fractal growth model for a lower water contents that is really close to the plastic limit (w_P). We previously mentioned that this limit marks the transition between agglomerates and dough regime under the effect of a modification in the mechanical behaviour.

5. Conclusion

During wet agglomeration of powders in a low shear mixer, the evolution of granulometric and hydro-textural parameters of the agglomerates during wetting were studied for three different products. Solid volume fraction, saturation degree and water content were measured at the agglomerate scale. These parameters were plotted on a phase diagram, called hydro-textural diagram which represents the elaboration path of agglomerates.

This experimental study makes it possible to observe that together with an increase in the diameter of agglomerates, the increase in water content lead to a decrease in their solid volume fraction. These two parameters (solid volume fraction and diameter) are perfectly correlated by a power law. This correlation is valid for all size fractions ranging between d_{25} and d_{75}. The exponent of this law (D_f) is the fractal dimension associated with this coalescence. Whatever the population fraction considered, D_f was proven to be constant. These results make it possible to hypothesize that agglomeration is a fractal structuring process.

The classical description of agglomeration mentions that it is composed of three successive stages: wetting/nucleation, consolidation/coalescence and growth, and breakage and attrition. This work brings complementary interpretations. The first stage of nucleation represents that during which the fractal growth patterns (the nuclei) are built. Experiments are in progress to study the influence of sprayed droplets size on nucleation stage and on the evolution of fractal structuring in its entirety. The second stage of growth by coalescence was proven to obey to a fractal behaviour. This experimental observation contradicts the classical description of agglomeration insofar as no consolidation phenomena (or increase in solid volume fraction) are observed during coalescence.

Currently, Eq. (9) is a retrodictive model. Five parameters (D_f, n, w_{sat}, d_{50}^N and ϕ_N) must be known so as to model the evolution of d_{50} with respect to the water content. These parameters can be determined only after agglomeration. Actually, works are in progress to correlate physico-chemical properties of the raw material (wetting liquid and powder) and process parameters to the value taken by these five parameters. The objective is to find statistical models linking the properties of the raw material to the parameters of Eq. (9) so as to predict the evolution of agglomerate size with respect to water content. Thus, this model could become an effective tool to fix the exact water content to add to a powder so as to obtain a specific size distribution. This tool could be very useful in several industrial fields using agglomeration as a first step. Actually, this process controls directly the efficiency of the production line because it can generate large amounts of recycling (*e.g.* up to 2.5 times the initial semolina flow in the case of couscous production).

References

[1] S.M. Iveson, J.D. Litster, K. Hapgood, B.J. Ennis, Nucleation, growth and breakage phenomena in agitated wet granulation processes: a review, Powder Technol. 117 (2001) 3–39.

[2] P.C. Knight, Structuring agglomerated products for improved performance, Powder Technol. 119 (2001) 14–25.

[3] A.B. Yu, N. Standish, L. Lu, Coal agglomeration and its effects on bulk density, Powder Technol. 82 (1995) 177–189.

[4] T. Ruiz, M. Delalonde, B. Bataille, G. Baylac, C. Dupuy de Crescenzo, Texturing unsaturated granular media submitted to compaction and kneading processes, Powder Technol. 154 (2005) 43–53.

[5] D.G. Bika, M. Gentzler, J.N. Michaels, Mechanical properties of agglomerates, Powder Technol. 117 (2001) 98–112.

[6] B.F.C. Laurent, Structure of powder flow in a planetary mixer during wet mass granulation, Chem. Eng. Sci. 60 (2005) 3805–3816.

[7] S. Galland, T. Ruiz, M. Delalonde, A. Krupa, B. Bataille, Texturing the spherical granular system: influence of the spheronisation stage, Powder Technol. 157 (2005) 156–162.

[8] S. Galland, T. Ruiz, M. Delalonde, Twin product/process approach for pellet preparation by extrusion/spheronisation: part I: hydro-textural aspects, Int. J. Pharm. 337 (2007) 239–245.

[9] T. Schaefer, C. Mathiesen, Melt pelletization in a high shear mixer. IX. Effects of binder particle size, Int. J. Pharm. 139 (1996) 139–148.

[10] R.D. Holtz, W.D. Kovacs, An Introduction to Geotechnical Engineering, Prentice-Hall Inc., Englewood Cliffs, 1981.

[11] D. Geldart, Types of gas fluidisation, Powder Technol. 7 (1973) 285–292.

[12] M.J. Hounslow, M. Oullion, G.K. Reynolds, Kinetic models for granule nucleation by the immersion mechanism, Powder Technol. 189 (2009) 177–189.

[13] C. Proust, A. Jullien, L. Le Forestier, Détermination indirecte des limites d'Atterberg par gravimétrie dynamique, C. R. Geosci. 336 (2004) 1233–1238.

[14] R. Botet, Les fractales en Physique, Techniques de l'Ingénieur, traité Physique Chimie, 2001, article AF 4500.

[15] R. Jullien, R. Botet, Aggregation and Fractal Aggregates, World Scientific, Singapore, 1987.

[16] D. Stauffer, H.E. Stanley, A. Lesne, Cours de Physique. De Newton à Mandelbrot, Springer-Verlag, France, 1999, pp. 271–313.

[17] T. Vicesk, Fractal models for diffusion-controlled aggregation, J. Phys. A 16 (1983) 647–650.

[18] E. Rondet, Texturation capillaire de milieux granulaires humides, Thèse de Doctorat, Université Montpellier II, 2008, http://tel.archives-ouvertes.fr/tel-00330501/fr/.